

Stable non-Fermi liquid fixed point at the onset of incommensurate $2k_F$ charge density wave order

Ipsita Mandal*

*Department of Physics, Shiv Nadar Institution of Eminence (SNIOE),
Gautam Buddha Nagar, Uttar Pradesh 201314, India*

*and
Freiburg Institute for Advanced Studies (FRIAS),
University of Freiburg, D-79104 Freiburg, Germany*

We consider the emergence of a non-Fermi liquid fixed point in a two-dimensional metal, at the onset of a quantum phase transition from a Fermi liquid state to an incommensurate charge density wave (CDW) ordered phase. The momentum of the CDW boson is centred at the wavevector \mathbf{Q} , which connects a single pair of antipodal points on the Fermi surface with antiparallel tangent vectors. We employ the dimensional regularization technique in which the co-dimension of the Fermi surface is extended to a generic value, while keeping the dimension of the Fermi surface itself fixed at one. Although the system is strongly coupled at dimension $d = 2$, the interactions become marginal at the upper critical dimension $d = d_c$, whose value is found to be $5/2$. Using a controlled perturbative expansion in the parameter $\epsilon = d_c - d$, we compute the critical exponents of the stable infrared fixed point characterizing the quantum critical point. The scalings of the original theory are determined by setting $\epsilon = 1/2$, where the fermion self-energy is seen to scale with the frequency with a fractional power law of $2/3$, which is the telltale signature of a typical non-Fermi liquid phase.

Contents

I. Introduction	1
II. Model	3
III. One-loop self-energies and dimensional regularization	4
A. One-loop boson self-energy	5
B. One-loop fermion self-energy	7
1. Computation of $\mathbf{\Gamma}$ -dependent part	7
2. Computation of γ_{d-1} -dependent part	8
C. One-loop vertex correction	9
IV. Renormalization Group flows under minimal subtraction scheme	9
A. RG flow equations from one-loop results	10
B. Stable fixed points	12
V. Discussions and outlook	13
References	14

I. Introduction

While Landau's Fermi liquid theory has been incredibly successful in describing normal metals, there exists an extensive number of metallic states where the framework fails. Although of widely different origins, these systems are widely known as non-Fermi liquids. A finite density of nonrelativistic fermions interacting with transverse $U(1)$ gauge field bosons was the first model, considered by Holstein *et al.* [1] to study the effects of the electromagnetic fields on a metal, to exhibit a non-Fermi liquid character. Subsequently, it was realized that similar behaviour is found for finite-density fermions coupled with massless order parameter bosons at quantum critical points [2–31] or artificial gauge field(s) emerging in various kinds of scenarios [32–39]. While the Landau quasiparticles provide a natural single-particle basis for writing down the corresponding low-energy quantum field theories (QFTs) on the merit of being long-lived excitations in a Landau Fermi liquid, they are destroyed by the strong interactions between the soft fluctuations of the Fermi surface and the gapless

* ipsita.mandal@snu.edu.in

bosonic quantum fields in the scenarios described above. Since these are fundamentally strongly-interacting theories, it is a challenging task to build a controlled approximation amenable to theoretical analysis. As a result, there have been intensive efforts to devise QFT frameworks to explain the emergent physical characteristics of these non-Fermi liquid systems [1, 2, 7, 17, 19–31, 35, 38–54]. In two spatial dimensions, the corresponding theories are genuinely strongly interacting, while in three dimensions, they emerge as marginal Fermi liquids [20, 53]. Analogous situations arise in two-dimensional (2d) and three-dimensional (3d) semimetals, where a non-Fermi liquid state emerges when the chemical potential cuts a band-crossing point giving rise to a Fermi point (rather than a Fermi surface) and a long-ranged (i.e., unscreened) Coulomb potential is switched on [55–65].

For non-Fermi liquids arising at quantum critical points, there are two types of order parameter bosons: (1) cases where the critical bosonic field is centred about zero momentum, inducing the quasiparticles to lose coherence across the entire Fermi surface [2–24]; (2) the momentum of the quantum field describing the bosonic degrees of freedom is centred around a finite wavevector equal to \mathcal{Q} , which connects points on the Fermi surface (commonly known as *hot-spots*), such that the non-Fermi liquid behaviour emerges locally in the vicinity of the hot-spots [2, 26–31, 52]. Examples in the first category include the Ising-nematic critical point, while the second one include ordering transitions to phases like spin density wave (SDW), charge density wave (CDW) [25–31], and the Fulde-Ferrell-Larkin-Ovchinnikov (FFLO) states [52].

The CDW (SDW) bosons with $\mathcal{Q} \neq 0$ give rise to instabilities involving charge (magnetic) order, where the charge (spin) density spontaneously breaks translational symmetries and develops a density modulation equal to $\mathcal{Q} \neq 0$. There are two distinct categorizations depending on the nature of the wavevector: (1) whether it is commensurate or incommensurate; (2) whether \mathcal{Q} is a nesting vector of the Fermi surface or not. While the so-called commensurate wavevectors can be written as a linear combination \mathbf{G} of the reciprocal lattice vectors $\{\mathcal{R}\}$ with rational coefficients, we cannot do the same for the incommensurate wavevectors. Clearly, there are infinitely many possible rational coefficients, but the quantitative effects of commensurability decrease with the size of their denominators. For the special situation of \mathcal{Q} equalling a nesting vector connecting two points on the Fermi surface with antiparallel Fermi velocities (or, equivalently, tangent vectors), the spin and charge orderings feature a well-known singularity caused by an enhanced phase space for low-energy particle-hole excitations. In an inversion-symmetric crystal with the valence band dispersion $\xi(\mathbf{k})$, the nesting vectors \mathcal{Q} are given by the condition $\xi(\mathcal{Q}/2 + \mathbf{G}/2) = \xi_{k_F}$, where ξ_{k_F} is the Fermi energy. The nesting-vector nature of \mathcal{Q} , coupled with inversion symmetry, implies that $|\mathcal{Q}| = 2k_F$, where k_F is the local radius of curvature/reciprocal of curvature of the Fermi surface (i.e., the magnitude of the local Fermi momentum vector). This results from the fact that the two hot-spots are related by inversion symmetry and, hence, both have the same value of k_F . The $2k_F$ -wavevector instabilities are ubiquitous in 2d systems exhibiting high-temperature superconductivity — for example, (1) the ground state of the 2d Hubbard model at half-filling of the conduction band exhibits an SDW instability at a $2k_F$ -wavevector [66, 67]; (2) d-wave bond charge order, triggered by antiferromagnetic fluctuations, in models for cuprate superconductors occurs naturally at $2k_F$ -wavevectors [25, 68]. We would like to emphasize that such a nesting vector causes a partial nesting of the Fermi surface, which is distinct from the perfect-nesting cases when slices (and not just discrete points) of a Fermi surface are connected by the same nesting vector. The evidence of incommensurate CDW orderings has been reported in materials like NbSe₂ and TaS₂ [69, 70], VSe₂ [71], SmTe₃ [72], and TbTe₃ [73]. In some of these compounds, the CDW transition temperature can be tuned close to zero Kelvin by applying high pressure, unravelling a putative quantum critical point at the onset of the CDW ordering [74]. Such observations indicate the importance of a theoretical understanding of quantum critical points involving incommensurate $2k_F$ -wavevector instabilities.

In this paper, we consider a pair of antipodal points on a 1d Fermi surface (of a 2d metal) with parallel tangent vectors interacting with an order parameter boson, whose condensation gives rise to an incommensurate CDW ordered phase [75–77]. The CDW boson becomes massless right at the quantum critical point, giving rise to strong quantum fluctuations. The physical picture here is that the CDW boson drives the system across a quantum phase transition to an ordered state, where the electron density spontaneously breaks translational symmetries and develops a density modulation with a wave vector \mathcal{Q} that is incommensurate with the underlying reciprocal lattice vectors. For the sake of definiteness, we choose $\mathcal{Q} = 2k_F \hat{x}$, without any loss of generality.

To deal with the QFT describing the above system, we implement the analytic approach of dimensional regularization [19–23, 52, 53, 78], in which the co-dimension of the Fermi surface is increased (as a mathematical tool) with the aim to obtain the value of the upper critical dimension $d = d_c$. Since d_c is the dimension at which the interactions become marginal, we succeed in formulating a controlled perturbative approximation, although the quasiparticle-description has broken down. The critical exponents and various physical properties can now be calculated in a systematic expansion involving the perturbative parameter $\epsilon = d_c - 2$. Halbinger *et al.* [77] have considered this incommensurate CDW problem by employing the same methodology, and have found that the fermion-boson interactions lead to a stable non-Fermi liquid fixed point. Furthermore, their results show that the resulting critical Fermi surface is flattened at the hot-spots. However, they arrived at their conclusions from some inaccurate computations, which, in addition to other results, could not find the correct critical dimension $d_c = 5/2$. They carried out their computations assuming that d_c is equal to $5/2$, predicting that it would be obtained at the two-loop order. Consequently, their answers do not include the all-important frequency dependence of $\text{sgn}(k_0)|k_0|^{2/3}$ for the fermion self-energy, which is predicted in the earlier (uncontrolled) random phase approximation (RPA) calculations [75, 76]. In order to address these inadequacies, the analysis via the dimensional regularization scheme must be reexamined, if only to put it on a firmer basis.

The paper is organized as follows. In Sec. II, we introduce the effective low-energy Euclidean action in the Matsubara

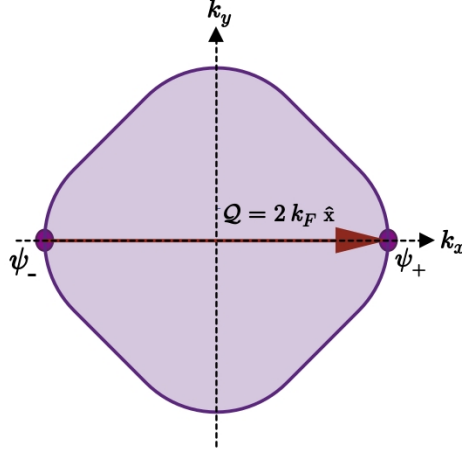


FIG. 1. Schematics of the one-dimensional Fermi surface with two hot-spots connected by the wavevector $\mathcal{Q} = 2 k_F \hat{x}$ (indicated by the red arrow), which is incommensurate with the underlying reciprocal lattice vectors. The fermionic fields in the vicinity of the right and left hot-spots are designated as ψ_+ and ψ_- , respectively. They interact with the CDW order parameter bosonic fields whose momenta are centred at \mathcal{Q} .

frequency space, describing the fermionic excitations at the two hot-spots of the Fermi surface interacting with the CDW boson fluctuations. The original theory is embedded in $d = 2$ spatial dimensions. We also explain how to generalize the theory to a generic value of d by increasing the number of dimensions perpendicular to the 1d Fermi surface, as this will allow us to identify the upper critical dimension d_c and, subsequently, to regularize the theory via the renormalization group (RG) procedure. Sec. III is devoted to the derivations of the bosonic and fermionic self-energies, and showing that d_c comes out to be $5/2$. Using the one-loop results, the RG flow equations are determined in Sec. IV by absorbing the ultraviolet (UV) divergences into singular counterterms. We discuss the nature of the fixed points in the infrared (IR) limit and show that the system flows to a stable non-Fermi liquid point. Finally, we conclude with the relevant discussions in Sec. V, comparing our computations and results with earlier works. The appendix shows a part of the computations of the fermion self-energy.

II. Model

We consider the low-energy QFT action describing finite-density fermions confined to two spatial dimensions, and interacting with an incommensurate CDW order parameter with momentum centred at $\mathcal{Q} = 2 k_F \hat{x}$. Thus, the nesting vector \mathcal{Q} connects two hot-spots on the Fermi surface located along the x -axis, as shown in Fig. 1. In $(2+1)$ -dimensions, the effective action describing the electrons near the hot-spots and the CDW order parameter mode is given by [75–77]

$$S = \sum_{s=\pm} \int_k \psi_s^\dagger(k) (-i k_0 + s k_1 + k_2^2) \psi_s(k) + \int_k \phi_+(k) (k_0^2 + k_1^2 + k_2^2) \phi_-(-k) + e \int_{k,q} \left[\phi_+(q) \psi_+^\dagger(k+q) \psi_-(k) + \phi_-(-q) \psi_-^\dagger(k-q) \psi_+(k) \right], \quad (1)$$

where $k = (k_0, \mathbf{k})$ denotes the three-vector comprising the Matsubara space frequency k_0 and the spatial momentum vector $\mathbf{k} = (k_1, k_2) \equiv (k_x, k_y)$, $\int_k \equiv \int dk_0 d^d \mathbf{k} / (2\pi)^{d+1}$, and $d = 2$ is the number of spatial dimensions. The fermionic degrees of freedom about the right and left hot-spots are denoted by $\psi_+(k)$ and $\psi_-(k)$, respectively. The fields $\phi_+(k)$ and $\phi_-(k)$ refer to the bosonic fluctuations carrying frequency k_0 and momenta $\mathcal{Q}/2 + \mathbf{k}$ and $-\mathcal{Q}/2 + \mathbf{k}$, respectively. The bosons are massless as we are considering the quantum critical point. To simplify notations, we have rescaled the fermionic momenta in a way such that the absolute value of the Fermi velocity is unity and the curvature of the Fermi surface is equal to 2 at the hot-spots. Although the bosonic velocity is in general distinct from that of the fermions, we have set the bare velocity of the bosons equal to unity as well. This is because the dynamics of the bosons at the critical point is dominated by the particle-hole excitations of the Fermi surface at low energies, and the actual value of the bosonic velocity does not matter in the low-energy effective theory.

In our action, since the Fermi surface is locally parabolic, we can set the scaling dimensions of k_1 and k_2 are equal to 1 and $1/2$, respectively. In order to extract the critical scalings in a controlled approximation, we increase the co-dimensions of the Fermi surface [19, 28, 78] to eventually determine the upper critical dimension $d = d_c$, where the fermion self-energy

shows a logarithmic singularity. To preserve the analyticity of the theory in momentum space (alternatively, locality in real space) with generic co-dimensions, we introduce the two-component “spinors” [19–21, 52–54]

$$\Psi(k) = \begin{pmatrix} \psi_+(k) & \psi_-^\dagger(-k) \end{pmatrix}^T \quad \text{and} \quad \bar{\Psi} \equiv \Psi^\dagger \gamma_0, \quad (2)$$

and write an action that describes the 1d Fermi surface embedded in a d -dimensional momentum space:

$$\begin{aligned} S = & \int_k \bar{\Psi}(k) i (\mathbf{\Gamma} \cdot \mathbf{K} + \gamma_{d-1} \delta_k) \Psi(k) + \int_k (k_d^2 + \tilde{a} e_k) \phi_+(k) \phi_-(-k) \\ & - \frac{i e \mu^{x_e/2}}{2} \int_{k,q} \left[\phi_+(q) \bar{\Psi}(k+q) \gamma_0 \bar{\Psi}^T(-k) + \phi_-(-q) \Psi^T(q-k) \gamma_0 \Psi(k) \right], \\ x_e = & \frac{5}{2} - d, \quad \delta_k = k_{d-1} + k_d^2, \quad e_k = k_{d-1} + \frac{k_d^2}{2}. \end{aligned} \quad (3)$$

The $(d-1)$ -component vector $\mathbf{K} \equiv (k_0, k_1, \dots, k_{d-2})$ includes the frequency and the $(d-2)$ -components of the momentum vector due to the added co-dimensions. The original momentum components along the x - and y -directions have been relabelled as k_{d-1} and k_d , respectively. Hence, in the resulting d -dimensional momentum space, the set of components $\{k_1, \dots, k_{d-1}\}$ represents the $(d-1)$ the direction perpendicular to the Fermi surface, while k_d is along the parallel direction. Similarly, the vector of matrices $\mathbf{\Gamma} \equiv (\gamma_0, \gamma_1, \dots, \gamma_{d-2})$ has $(d-1)$ components representing the gamma matrices associated with k_0 and the extra co-dimensions. Ultimately, we are interested in continuing to $d = 2$, which implies that, in practice, it is sufficient to consider only the 2×2 gamma matrices $\gamma_0 = \sigma_y$ and $\gamma_{d-1} = \sigma_x$ in our computations.

In the purely bosonic part of the action, only the k_d^2 part of the kinetic term is retained, because $(|\mathbf{K}|^2 + k_{d-1}^2)$ is irrelevant under the scaling of the patch-theory formalism [2, 19–21, 52, 53, 77], where each of $\{\mathbf{K}, k_{d-1}\}$ has dimension unity and k_d has dimension $1/2$. Dependence on e_k in the bosonic propagator will be generated via the susceptibility, which is obtained from the dynamics of the strong particle-hole fluctuations. Anticipating this, we have already added the extra term $\tilde{a} e_k$, which will be generated in the RG process, and its has been dictated by the divergent term in the one-loop susceptibility calculated in the following subsection [see Eq. (13)]. In other words, we have simply included a term which will be generated via quantum corrections. This term has a mass dimension equal to unity, similar to the k_d^2 term, with a vanishing engineering dimension for \tilde{a} . If we do not include this term, the loop integrations involving the bosonic propagator will turn out to be infrared-divergent, and these divergences will be the mere artifacts of our dropping the irrelevant terms in the minimal local effective action (if it contains only the k_d^2 term). Finally, the engineering dimension of the fermion-boson coupling e is equal to $x_e/2$ — this observation has dictated us to introduce an explicit factor of a mass scale μ raised to the power $x_e/2$, chosen so as to ensure that e is dimensionless, which is the usual procedure followed in QFT calculations.

The emergent *sliding symmetry* in the Ising-nematic case [2, 19–21] forces the terms proportional to $[\bar{\Psi}(k) k_{d-1} \Psi(k)]$ and $[\bar{\Psi}(k) k_d^2 \Psi(k)]$ in Eq. (3) to renormalize in the same way. In other words, the fermion propagator depends on k_{d-1} and k_d^2 only through δ_k even after loop corrections. However, that is not the case here, and the renormalization process is not guaranteed to retain the sole dependence on δ_k . In other words, it is possible that the nature of the renormalized terms may turn out to be such that it leads to a flattening of the Fermi surface at the hot-spots, as found in the RPA calculations of Ref. [76]. Nevertheless, as we will see from our explicit calculations, the flattening does not show up in our one-loop level computations.

III. One-loop self-energies and dimensional regularization

The value of x_e tells us that the coupling constant e becomes marginal at the upper critical dimension $d_c = 5/2$. In other words, e is relevant for $d < 5/2$ and irrelevant for $d > 5/2$. Our aim is to access the interacting phase perturbatively in $d = 5/2 - \epsilon$, using ϵ as the perturbative parameter. In particular, this implies that at the end of our systematic ϵ -expansion, we have to set $\epsilon = 1/2$ for our original two-dimensional theory. Before embarking on deriving the RG flows, in this section, we compute the one-loop self-energies for the bosonic and fermionic degrees of freedom, which will feed into the equations necessary for determining the beta functions of the coupling constants e and \tilde{a} .

The bare fermion and boson propagators for the action defined in Eq. (3) are given by

$$\begin{aligned} G_{(0)}(k) & \equiv \langle \Psi(k) \bar{\Psi}(k) \rangle_0 = \frac{1}{i} \frac{\mathbf{\Gamma} \cdot \mathbf{K} + \gamma_{d-1} \delta_k}{|\mathbf{K}|^2 + \delta_k^2}, \quad D_{(0)}^+(k) \equiv \langle \phi^+(k) \phi^-(-k) \rangle_0 = \frac{1}{k_d^2 + \tilde{a} e_k}, \\ D_{(0)}^-(k) & \equiv \langle \phi^-(k) \phi^+(-k) \rangle_0 = D_{(0)}^+(k). \end{aligned} \quad (4)$$



FIG. 2. The one-loop diagrams for (a) the boson self-energy and (b) the fermion self-energy. Curves with arrows represent the bare fermion propagator $G_{(0)}$, whereas the wiggly lines represent the dressed bosonic propagator $D_{(1)}$.

A. One-loop boson self-energy

The one-loop boson self-energy [cf. Fig. 2(a)] is defined by

$$\Pi(k) = -\frac{e^2 \mu^{x_e}}{4} \times 2 \int_q \text{Tr} \left[\gamma_0 G_{(0)}(k) \gamma_0 G_{(0)}^T(k-q) \right]. \quad (5)$$

Using the commutation relations between the gamma-matrices, and the identities $\gamma_{d-1}^T = -\gamma_0 \gamma_{d-1} \gamma_0$ and $\Gamma^T = -\gamma_0 \Gamma \gamma_0$, we get

$$\Pi(k) = e^2 \mu^{x_e} \int_q \frac{\mathbf{Q} \cdot (\mathbf{Q} - \mathbf{K}) - \delta_q \delta_{k-q}}{(\mathbf{Q}^2 + \delta_q^2) [(\mathbf{Q} - \mathbf{K})^2 + \delta_{k-q}^2]}. \quad (6)$$

Noting that $\delta_{k-q} = k_{d-1} + q_{d-1} + (k_d - q_d)^2$, we first shift $q_{d-1} \rightarrow q_{d-1} - q_d^2$, and then use the Feynman parametrization to obtain

$$\begin{aligned} \Pi(k) &= e^2 \mu^{x_e} \int_q \int_0^1 dt \frac{|\mathbf{Q}|^2 - t(1-t)|\mathbf{K}|^2 - \tilde{e}_{kq} q_{d-1} + q_{d-1}^2}{\left[|\mathbf{Q}|^2 + t(1-t)|\mathbf{K}|^2 + t\tilde{e}_{kq}^2 + q_{d-1}^2 - 2t\tilde{e}_{kq} q_{d-1} \right]^2} \quad (\text{where } \tilde{e}_{kq} = k_{d-1} + k_d^2 - 2k_d q_d + 2q_d^2) \\ &= e^2 \mu^{x_e} \int d^{d-1} |\mathbf{Q}| dq_d \int_0^1 dt \frac{|\mathbf{Q}|^d}{2^d \pi^{\frac{d+1}{2}} \Gamma\left(\frac{d-1}{2}\right) \left[|\mathbf{Q}|^2 + t(1-t) \left(\tilde{e}_{kq}^2 + |\mathbf{K}|^2 \right) \right]^{3/2}} \\ &= e^2 \mu^{x_e} \int dq_d \frac{2^{1-2d} \csc\left(\frac{d\pi}{2}\right) \left(\tilde{e}_{kq}^2 + |\mathbf{K}|^2 \right)^{\frac{d-2}{2}}}{\pi^{\frac{d-1}{2}} \Gamma\left(\frac{d-1}{2}\right)}. \end{aligned} \quad (7)$$

Changing variables to $u = \sqrt{2} q_d - k_d / \sqrt{2}$ with the Jacobian factor $1/\sqrt{2}$, we get

$$\Pi(k) = e^2 \mu^{x_e} \int_0^\infty du \frac{2^{\frac{3}{2}-2d} \csc\left(\frac{d\pi}{2}\right) \left[(u^2 + e_k)^2 + |\mathbf{K}|^2 \right]^{\frac{d-2}{2}}}{\pi^{\frac{d-1}{2}} \Gamma\left(\frac{d-1}{2}\right)}. \quad (8)$$

Since the bare susceptibility at zero temperature diverges at the nesting vector \mathbf{Q} , the well-defined self-energy is given by subtracting off the singular contribution for this momentum, which translates to

$$\tilde{\Pi}(k) = \Pi(k) - \Pi(0) = \frac{2^{\frac{3}{2}-2d} \csc\left(\frac{d\pi}{2}\right) e^2 \mu^{x_e}}{\pi^{\frac{d-1}{2}} \Gamma\left(\frac{d-1}{2}\right)} I_\Pi(k, d), \quad (9)$$

where (after changing variables as $z = u^2 + e_k$)

$$\begin{aligned}
I_{\Pi}(k, d) &\equiv \int_{e_k}^{\infty} dz \frac{(z - e_k)^{2-d} - [z^2 + |\mathbf{K}|^2]^{\frac{2-d}{2}}}{2\sqrt{z - e_k} [z^2 + |\mathbf{K}|^2]^{\frac{2-d}{2}} (z - e_k)^{2-d}} \\
&= \begin{cases} \frac{\Gamma(d-1)(-e_k)^{d-\frac{3}{2}}}{2} \left[\frac{\Gamma(\frac{3-d}{2}) {}_2F_1\left(\frac{3-2d}{4}, \frac{5-2d}{4}; \frac{3-d}{2}; -\frac{|\mathbf{K}|^2}{e_k^2}\right)}{\sqrt{\pi}} + \frac{{}_2F_1\left(\frac{1}{2}, 1; d; 1\right)}{\Gamma(d)} \right] \\ + \frac{|\mathbf{K}|^d {}_3F_2\left(\frac{3}{4}, 1, \frac{5}{4}; \frac{3}{2}, \frac{d}{2}+1; -|\mathbf{K}|^2/e_k^2\right)}{4d(-e_k)^{3/2}} + \frac{\pi^{3/2} |\mathbf{K}|^{d-1} \sec\left(\frac{d\pi}{2}\right) {}_2F_1\left(\frac{1}{4}, \frac{3}{4}; \frac{d+1}{2}; -|\mathbf{K}|^2/e_k^2\right)}{4\sqrt{-e_k} \Gamma\left(\frac{2-d}{2}\right) \Gamma\left(\frac{d+1}{2}\right)} \\ + |\mathbf{K}|^{d-2} \sqrt{-e_k} {}_3F_2\left(\frac{1}{2}, 1, 1 - \frac{d}{2}; \frac{3}{4}, \frac{5}{4}; -\frac{e_k^2}{|\mathbf{K}|^2}\right) + \frac{(-e_k)^{d-\frac{3}{2}}}{3-2d} & \text{for } e_k < 0 \\ \frac{\sqrt{\pi} e_k^{d-\frac{3}{2}} \Gamma\left(\frac{3-d}{2}\right) {}_2F_1\left(\frac{3-2d}{4}, \frac{5-2d}{4}; \frac{3-d}{2}; -|\mathbf{K}|^2/e_k^2\right)}{2\Gamma(2-d)} & \text{for } e_k > 0. \end{cases} \quad (10)
\end{aligned}$$

Note that the zeroes coming from $1/\Gamma\left(\frac{2-d}{2}\right)$ and $1/\Gamma(2-d)$ at $d = 2$ are cancelled by the factor $\csc\left(\frac{d\pi}{2}\right)$ present in Eq. (9).

The leading order terms obtained in the limit $|\mathbf{K}|^2/e_k^2 \ll 1$ are found to be:

$$\begin{aligned}
I_{\Pi}(k, d) &= \begin{cases} \frac{\Gamma(d-1)(-e_k)^{d-\frac{3}{2}}}{2} \left[\frac{{}_2\tilde{F}_1\left(\frac{1}{2}, 1; d; 1\right)}{\Gamma(d)} + \frac{\Gamma\left(\frac{3-d}{2}\right)}{\sqrt{\pi}} + \frac{\sqrt{\pi}}{\Gamma\left(d-\frac{1}{2}\right)} \right] + \frac{(-e_k)^{d-\frac{3}{2}}}{3-2d} + \frac{\pi^{3/2} |\mathbf{K}|^{d-1} \sec\left(\frac{d\pi}{2}\right)}{2\sqrt{-e_k} \Gamma\left(\frac{2-d}{2}\right) \Gamma\left(\frac{d+1}{2}\right)} + \mathcal{O}\left(\frac{|\mathbf{K}|^d}{(-e_k)^{3/2}}\right) & \text{for } e_k < 0 \\ \frac{\sqrt{\pi} \Gamma\left(\frac{3-d}{2}\right) e_k^{d-\frac{3}{2}}}{2\Gamma(2-d)} + \frac{\sqrt{\pi} \Gamma\left(\frac{7}{2}-d\right) |\mathbf{K}|^2}{4(d-3)\Gamma(2-d)e_k^{\frac{7-2d}{2}}} + \mathcal{O}\left(\frac{|\mathbf{K}|^4}{e_k^{11/2-d}}\right) & \text{for } e_k > 0. \end{cases} \quad (11)
\end{aligned}$$

Finally, expanding in ϵ for $d = 5/2 - \epsilon$, we get

$$\begin{aligned}
&\left[\mu^{x_e} \frac{2^{\frac{3}{2}-2d} \csc\left(\frac{d\pi}{2}\right)}{\pi^{\frac{d-1}{2}} \Gamma\left(\frac{d-1}{2}\right)} \times I_{\Pi}(k, d) \right] \Big|_{d=5/2-\epsilon} \\
&= \begin{cases} -\frac{e_k \left(\frac{\mu}{|e_k|}\right)^\epsilon}{32 \pi^{3/4} \Gamma(3/4) \epsilon} - \frac{\pi - 2 \ln(32\pi) + 2\gamma_E + 4}{128 \pi^{3/4} \Gamma\left(\frac{3}{4}\right)} e_k \left(\frac{\mu}{|e_k|}\right)^\epsilon - \frac{\pi^{3/4} \frac{|\mathbf{K}|^{\frac{3}{2}}}{\sqrt{|e_k|}} \left(\frac{\mu}{|\mathbf{K}|}\right)^\epsilon}{32 \sqrt{2} \Gamma^2(3/4) \Gamma(7/4)} + \mathcal{O}(\epsilon) & \text{for } e_k < 0 \\ -\frac{e_k \left(\frac{\mu}{e_k}\right)^\epsilon}{32 \pi^{3/4} \Gamma(3/4) \epsilon} - \frac{3\pi + 2 \ln(32\pi) - 2\gamma_E - 4}{128 \pi^{3/4} \Gamma(3/4)} e_k \left(\frac{\mu}{e_k}\right)^\epsilon - \frac{|\mathbf{K}|^2 \left(\frac{\mu}{e_k}\right)^\epsilon}{32 \pi^{3/4} \Gamma(3/4)} + \mathcal{O}(\epsilon) & \text{for } e_k > 0, \end{cases} \quad (12)
\end{aligned}$$

where γ_E is the Euler-Mascheroni constant. It is important to note here that the loop integral has an upper critical dimension at $d = 3/2$ and, as a result, it shows a pole in ϵ also at $d = 5/2 - \epsilon$. As such, these terms in the one-loop corrected action will be irrelevant, which is reflected by the that they have a scaling dimension equal to $(1-\epsilon)$ at $d = 5/2 - \epsilon$.

From our analysis above, we conclude that the self-energy correction in Eq. (9) is given by

$$\tilde{\Pi}(k) = -e^2 \left[\frac{1}{32 \pi^{3/4} \Gamma(3/4) \epsilon} + a \right] e_k - \frac{e^2 \mu^{x_e} b |\mathbf{K}|^{d-1}}{\sqrt{|e_k|}} \Theta(-e_k) - \frac{e^2 c |\mathbf{K}|^2}{|e_k|^{7/2-d}} \Theta(e_k), \quad (13)$$

where

$$\begin{aligned}
a &= \frac{\pi - 2 \ln(32\pi) + 2\gamma_E + 4}{128 \pi^{3/4} \Gamma\left(\frac{3}{4}\right)} \Theta(-e_k) + \frac{3\pi + 2 \ln(32\pi) - 2\gamma_E - 4}{128 \pi^{3/4} \Gamma(3/4)} \Theta(e_k), \\
b &= \frac{\pi^{3/4}}{32 \sqrt{2} \Gamma^2(3/4) \Gamma(7/4)}, \quad c = \frac{1}{32 \pi^{3/4} \Gamma(3/4)}. \quad (14)
\end{aligned}$$

We note that the bare boson propagators D_{\pm} are still independent of \mathbf{K} , the loop integrations involving it are ill-defined unless one resums a series of diagrams that provides a nontrivial dispersion along these frequency and momentum components. Hence, in all loop calculations involving the boson propagators, we include the lowest order fine correction $\Pi_{\text{LD}}(k)$ from the one-loop self-energy, which is proportional to $|\mathbf{K}|^{d-1}/\sqrt{|e_k|}$. Therefore, both for the $\phi_+(k)$ and $\phi_-(k)$ bosonic fields, we use the dressed propagator

$$D_{(1)}(k) = \frac{1}{\left[D_{(0)}^+(k) \right]^{-1} - \Pi_{\text{LD}}(k)} = \frac{1}{k_d^2 + \tilde{a} e_k + \frac{b e^2 \mu^{x_e} |\mathbf{K}|^{d-1} \Theta(-e_k)}{\sqrt{|e_k|}}}, \quad (15)$$

which is equivalent to rearranging the perturbative loop-expansions such that the one-loop finite part of the boson self-energy, dependent on \mathbf{K} , is included at the zeroth order. We would like to emphasize that $\Pi_{\text{LD}}(k)$ is the so-called *Landau-damped term* which leads to the signature $\text{sgn}(k_0)|k_0|^{2/3}$ -dependence of the fermion self-energy, characterizing the non-Fermi liquid behaviour in various quantum critical systems [2, 19–21, 25, 52, 53, 77]. The Landau-damped part also plays the most significant role in inducing unconventional superconductivity in this kind of non-Fermi liquid systems [23, 24, 48, 49, 79].

B. One-loop fermion self-energy

The fermion self-energy [cf. Fig. 2(b)] is given by the integral

$$\Sigma(k) = e^2 \mu^{x_e} \int_q \gamma_0 G_{(0)}^T(q-k) \gamma_0 D_{(1)}(q) = i \Sigma_1(k) \Gamma \cdot \mathbf{K} + i \Sigma_2(k) \gamma_{d-1}, \quad (16)$$

where

$$\Sigma_1(k) = -\frac{e^2 \mu^{x_e}}{|\mathbf{K}|^2} \int_q \frac{\mathbf{K} \cdot (\mathbf{Q} - \mathbf{K})}{(\mathbf{Q} - \mathbf{K})^2 + \delta_{q-k}^2} D_{(1)}(q) \quad (17)$$

and

$$\Sigma_2(k) = e^2 \mu^{x_e} \int_q \frac{\delta_{q-k}}{(\mathbf{Q} - \mathbf{K})^2 + \delta_{q-k}^2} D_{(1)}(q). \quad (18)$$

The steps to compute these two parts have been explained in the next two subsections, which can be skipped if the reader is not interested in the tedious intermediate steps. For their benefit, we state here the final result. Setting $d = d_c - \epsilon$, we get the singular part to be

$$\Sigma(k) = -\frac{e^{4/3} \mathcal{U}_1}{(2 - \tilde{a})^{2/3} \epsilon} i (\Gamma \cdot \mathbf{K}) + \mathcal{O}(\epsilon^0), \quad \mathcal{U}_1 = \frac{\sqrt{2} \Gamma(\frac{5}{4})}{3 \sqrt{3} \pi^{7/4} b^{1/3}}, \quad (19)$$

where the divergence is parametrized by a pole at $\epsilon = 0$.

1. Computation of Γ -dependent part

The leading order dependence of $\Sigma_1(k)$ on \mathbf{K} can be extracted by setting the external momentum components k_d and k_{d-1} to zero. Hence, we will evaluate

$$\Sigma_1(\mathbf{K}, 0, 0) = \frac{e^2 \mu^{x_e}}{|\mathbf{K}|^2} \int_q \frac{\mathbf{K} \cdot (\mathbf{K} - \mathbf{Q})}{(\mathbf{Q} - \mathbf{K})^2 + \delta_q^2} \times \frac{1}{q_d^2 + \tilde{a} e_q + e^2 \mu^{x_e} b |\mathbf{Q}|^{d-1} \Theta(-e_q) / \sqrt{|e_q|}}. \quad (20)$$

Changing the description to q_d and e_q as integration variables, and dividing into the parts $e_q < 0$ and $e_q > 0$ as $\Sigma_1(\mathbf{K}, 0, 0) = I_1 + I_2$, we have

$$\begin{aligned} I_1 &= \frac{e^2 \mu^{x_e}}{|\mathbf{K}|^2} \int_{e_q < 0} \frac{d^{d-1} \mathbf{Q} dq_d de_q}{(2\pi)^{d+1}} \frac{-\mathbf{K} \cdot (\mathbf{Q} - \mathbf{K})}{(\mathbf{Q} - \mathbf{K})^2 + (e_q + q_d^2/2)^2} \frac{1}{q_d^2 + \tilde{a} e_q + e^2 \mu^{x_e} b |\mathbf{Q}|^{d-1} / \sqrt{|e_q|}} \\ &= \frac{e^2 \mu^{x_e}}{|\mathbf{K}|^2} \int_0^\infty \frac{du}{\sqrt{u/2}} \int_0^\infty de_q \int_{-\infty}^\infty \frac{d^{d-1} \mathbf{Q}}{(2\pi)^{d+1}} \frac{\mathbf{K}^2 - \mathbf{K} \cdot \mathbf{Q}}{(\mathbf{Q} - \mathbf{K})^2 + (u - e_q)^2} \frac{1}{2u - \tilde{a} e_q + e^2 \mu^{x_e} b |\mathbf{Q}|^{d-1} / \sqrt{e_q}} \quad [\text{where } 2u = q_d^2], \end{aligned} \quad (21)$$

and

$$\begin{aligned} I_2 &= \frac{e^2 \mu^{x_e}}{|\mathbf{K}|^2} \int_{e_q > 0} \frac{d^{d-1} \mathbf{Q} dq_d de_q}{(2\pi)^{d+1}} \frac{-\mathbf{K} \cdot (\mathbf{Q} - \mathbf{K})}{(\mathbf{Q} - \mathbf{K})^2 + (e_q + q_d^2/2)^2} \frac{1}{q_d^2 + \tilde{a} e_q} \\ &= \frac{e^2 \mu^{x_e}}{|\mathbf{K}|^2} \int_{e_q > 0} \frac{d^{d-1} \mathbf{Q} dq_d de_q}{(2\pi)^{d+1}} \frac{-\mathbf{K} \cdot \mathbf{Q}}{\mathbf{Q}^2 + (e_q + q_d^2/2)^2} \frac{1}{q_d^2 + \tilde{a} e_q} = 0. \end{aligned} \quad (22)$$

The integral I_1 cannot be evaluated exactly and we need to make some reasonable approximations to extract the leading order corrections. We note that the first factor of the integrand tells us that the dominant contribution is

concentrated around the region $|\mathbf{Q}| \sim |\mathbf{K}|$ and $u \sim e_q$. As for the second factor, the dominant contribution comes from $e_q \sim |\mathbf{Q}|^{2(d-1)/3} \sim |\mathbf{K}|^{2(d-1)/3}$. Since $|\mathbf{K}|^{2(d-1)/3} \gg |\mathbf{K}|$ for small $|\mathbf{K}|$ close to zero and $2(d-1)/3 < 1$, we can substitute $u \sim e_q$ in the \sqrt{u} factor in the overall denominator and the $2u$ term in the denominator of the second factor, and extend the lower limit of the integral over u to $-\infty$, leading to

$$\begin{aligned}
I_1 &\simeq \frac{e^2 \mu^{x_e}}{|\mathbf{K}|^2} \int_{-\infty}^{\infty} \frac{d^{d-1} \mathbf{Q} du}{(2\pi)^{d+1}} \int_{e_q > 0} \frac{de_q}{\sqrt{e_q/2}} \frac{\mathbf{K} \cdot (\mathbf{K} - \mathbf{Q})}{(\mathbf{Q} - \mathbf{K})^2 + u^2} \frac{1}{(2 - \tilde{a}) e_q + e^2 \mu^{x_e} b |\mathbf{Q}|^{d-1} / \sqrt{e_q}} \quad [\text{shifting } u \rightarrow u + e_q] \\
&= \frac{e^2 \mu^{x_e}}{|\mathbf{K}|^2} \int_{-\infty}^{\infty} \frac{d^{d-1} \mathbf{Q} du}{(2\pi)^{d+1}} \int_{e_q > 0} de_q \frac{\mathbf{K} \cdot (\mathbf{K} - \mathbf{Q})}{(\mathbf{Q} - \mathbf{K})^2 + u^2} \frac{\sqrt{2}}{(2 - \tilde{a}) e_q^{3/2} + e^2 \mu^{x_e} b |\mathbf{Q}|^{d-1}} \\
&= -\frac{e^{4/3} \Gamma(\frac{5-2d}{6}) \Gamma(\frac{d}{2}) \Gamma(\frac{d+2}{6})}{2^{\frac{4d-1}{6}} \pi^{\frac{d+1}{2}} \times 3 \sqrt{3} (2 - \tilde{a})^{2/3} b^{1/3} \Gamma(\frac{5d-2}{6})} \left(\frac{\mu}{|\mathbf{K}|} \right)^{\frac{2x_e}{3}}. \quad (23)
\end{aligned}$$

The integral blows up at $d = 5/2$, which thus gives us the value of the upper critical dimension d_c . The fermion-boson coupling e is irrelevant for $d > d_c$, relevant for $d < d_c$, and marginal for $d = d_c$. This allows us to access the strongly interacting non-Fermi liquid state perturbatively, in a controlled approximation, using $d = 5/2 - \epsilon$, where ϵ serves as the perturbative/small parameter. In our dimensional regularization scheme, the divergence appears as $\sim \epsilon^{-1}$, with the $\Gamma(\frac{5-2d}{6})$ factor having a pole at $d = d_c$. We also note that this term produces the behaviour of the fermion self-energy as $\sim \text{sgn}(k_0) |k_0|^{2/3}$ at $d = 2$, which matches with the uncontrolled RPA result [75, 76]. We would like to point out that the correct k_0 -dependence of Σ could be captured only because we have included the crucial Landau damping term in the dressed bosonic propagator $D_{(1)}$. The $|k_0|^{2/3}$ -scaling was missed in Ref. [77] due to the non-inclusion of Π_{LD} .

2. Computation of γ_{d-1} -dependent part

The leading order dependence of $\Sigma_2(k)$ on k_d and k_{d-1} can be extracted by setting $\mathbf{K} = 0$. Hence, we will evaluate

$$\Sigma_2(\mathbf{0}, k_d, k_{d-1}) = e^2 \mu^{x_e} I_3, \quad I_3 = \int_q \frac{\delta_{q-k}}{\mathbf{Q}^2 + \delta_{q-k}^2} \times \frac{1}{q_d^2 + \tilde{a} e_q + e^2 \mu^{x_e} b |\mathbf{Q}|^{d-1} \Theta(-e_q) / \sqrt{|e_q|}}, \quad (24)$$

where $\delta_{q-k} = q_{d-1} - k_{d-1} + k_d^2 + q_d^2 - 2k_q q_d$. We note that the first factor of the integrand sets the condition that the dominant contributions must come when $|\mathbf{Q}| \sim 0$. This immediately tells us that, in the denominator of the second factor, the term proportional to b is subleading. Hence, to extract the leading order contribution we can set it to zero. In the appendix, we show that the subleading order term turns out to be proportional to $b^{1/3}$ and is not singular at $d = d_c$. Therefore, we calculate the approximate integral

$$\begin{aligned}
I_3 &\simeq \int_q \frac{\delta_{q-k}}{\mathbf{Q}^2 + \delta_{q-k}^2} \times \frac{1}{q_d^2 + \tilde{a} e_q} \\
&= \int \frac{d^{d-1} \mathbf{Q} dq_d du}{(2\pi)^{d+1}} \frac{u - k_{d-1}}{[|\mathbf{Q}|^2 + (u - k_{d-1})^2]} \times \frac{2}{q_d^2 + \frac{2\tilde{a}}{2-\tilde{a}} (u - 2k_d q_d - k_d^2)} \quad [\text{where } u = \delta_q + 2k_d q_d + k_d^2]. \quad (25)
\end{aligned}$$

Using the identity

$$\int_{-\infty}^{\infty} \frac{dw}{w^2 + A} = \begin{cases} 0 & \text{for } \mathcal{A} < 0 \\ \frac{\pi}{\sqrt{\mathcal{A}}} & \text{for } \mathcal{A} > 0, \end{cases} \quad (26)$$

for the Cauchy principal value of the integral, the q_d -integral is performed first to obtain the form

$$\begin{aligned}
I_3 &= \int \frac{d^{d-1} \mathbf{Q} du}{(2\pi)^d} \frac{u - k_{d-1}}{[|\mathbf{Q}|^2 + (u - k_{d-1})^2]} \times \frac{\Theta(u - \frac{(2+\tilde{a})k_d^2}{2-\tilde{a}})}{(2 - \tilde{a}) \sqrt{u - \frac{(\tilde{a}+2)k_d^2}{2-\tilde{a}}}} \\
&= \int \frac{d^{d-1} \mathbf{Q} du}{(2\pi)^d} \frac{\frac{(2+\tilde{a})k_d^2}{2-\tilde{a}} + \tilde{u} - k_{d-1}}{[|\mathbf{Q}|^2 + \left(\frac{(\tilde{a}+2)k_d^2}{2-\tilde{a}} + \tilde{u} - k_{d-1}\right)^2]} \times \frac{\Theta(\tilde{u})}{(2 - \tilde{a}) \sqrt{\tilde{u}}} \quad [\text{where } \tilde{u} = u - \frac{(2 + \tilde{a}) k_d^2}{2 - \tilde{a}}] \\
&= \int_0^{\infty} \frac{d|\mathbf{Q}|}{\pi^{\frac{d-1}{2}}} \frac{1}{2d \sqrt{2 - \tilde{a}} \Gamma(\frac{d-1}{2}) |\mathbf{Q}|^{2-d}} \left[\frac{1}{\sqrt{(2 + \tilde{a}) k_d^2 - (2 - \tilde{a}) (k_{d-1} + i|\mathbf{Q}|)}} + \frac{1}{\sqrt{(2 + \tilde{a}) k_d^2 + (2 - \tilde{a}) (-k_{d-1} + i|\mathbf{Q}|)}} \right] \\
&= \frac{\sin(\frac{\pi d}{2}) \Gamma(\frac{3}{2} - d) \Gamma(\frac{d}{2})}{2 \pi^{\frac{d+1}{2}} (2 - \tilde{a})} \left[-e_k + \left(\frac{6 + \tilde{a}}{2 - \tilde{a}} \right) \frac{k_d^2}{2} \right]^{d-\frac{3}{2}}. \quad (27)
\end{aligned}$$

The factor $\Gamma(\frac{3}{2} - d)$ has a pole at $d = 3/2$, which shows that this term has (1) a logarithmic divergence at $d = 3/2$, and (2) a linear divergence at $d = 5/2$, when we translate the divergences in the language of the Wilsonian cutoff $\Lambda \sim \mu$. We need to treat this result carefully by remembering that, in the dimensional regularization procedure, UV divergences of all degrees show up as the poles of Γ -functions. The degree of divergence can be understood by using an explicit UV cut-off in the language of the Wilsonian RG, which is denoted here by Λ . Although this term will play an important role for analyzing UV-stable fixed points, it should be discarded here because we are considering the RG flows in the IR, and this term represents an IR-irrelevant operator for the theory in $d = 5/2 - \epsilon$.

Some more comments are in order. The situation above is similar to having a ϕ^6 -term in a ϕ^4 scalar field theory in $(3 + 1)$ -dimensions. A simple power counting of momenta arising in loop diagrams shows that adding a ϕ^6 -interaction vertex to a free scalar field theory gives an upper critical dimension of 3, while addition of a ϕ^4 -vertex has the upper critical dimension value of 4. Therefore, adding a ϕ^6 -vertex to the ϕ^4 theory in four spacetime dimensions makes the theory nonrenormalizable.

The above statements can also be quantified in an alternate way. Let us expand the expression in $\tilde{\epsilon}$, where $d = 3/2 - \tilde{\epsilon}$. Then we have

$$\Sigma_2 \Big|_{d=3/2-\tilde{\epsilon}} = \frac{e^2 \left[-e_k + \left(\frac{6+\tilde{a}}{2-\tilde{a}} \right) \frac{k_d^2}{2} \right]}{\sqrt{2} \pi^{5/4} (2 - \tilde{a}) \tilde{\epsilon}} \left[\frac{\mu}{-e_k + \left(\frac{6+\tilde{a}}{2-\tilde{a}} \right) \frac{k_d^2}{2}} \right]^{1+\tilde{\epsilon}} + \mathcal{O}(\tilde{\epsilon}^0), \quad (28)$$

which indicates that the term has a linear UV divergence at $d = 5/2$. Another crucial observation is that I_3 vanishes identically at $d = 2$. All these observations together dictate that there will be no contribution to the RG flows in the IR from this term and, hence, should not be included in the counterterms. Consequently, the flattening of the Fermi surface at the hot-spots, found in the RPA calculations [76], does not show up in our one-loop results.

C. One-loop vertex correction

It is not possible to get a one-loop vertex diagram and, hence, the corresponding correction is zero.

IV. Renormalization Group flows under minimal subtraction scheme

Eq. (3) is supposed to be the *physical action*, defined at an energy scale $\mu \sim \Lambda$, consisting of the fundamental Lagrangian with non-divergent quantities. However, we have seen that the loop integrals lead to divergent terms and, in order to cure it, we employ the renormalization procedure, using dimensional regularization as the regularization method. In our dimensional regularization formalism, the UV-divergent terms are the ones arising in the $\epsilon \rightarrow 0$ limit. We use the minimal subtraction (MS) renormalization scheme to control the UV divergences [80, 81], which involves cancelling the divergent parts of the loop-contributions via adding appropriate counterterms. More precisely, we adopt the modified minimal subtraction ($\overline{\text{MS}}$) scheme where, in addition to the divergent term, we absorb the universal term proportional to ϵ^0 (that always accompanies the term with the $1/\epsilon$ pole) into the corresponding counterterm.

The action, consisting of the counterterms to absorb the singular terms, takes the form:

$$\begin{aligned} S_{CT} = & \int_k \bar{\Psi}(k) i \left[A_1 \mathbf{\Gamma} \cdot \mathbf{K} + \gamma_{d-1} \left(A_2 e_k + A_3 \frac{k_d^2}{2} \right) \right] \Psi(k) + \int_k (A_4 k_d^2 + A_5 \tilde{a} e_k) \phi_+(k) \phi_-(-k) \\ & - \frac{i e \mu^{x_\epsilon/2}}{2} \int_{k,q} A_6 \left[\phi_+(q) \bar{\Psi}(k+q) \gamma_0 \bar{\Psi}^T(-k) + \phi_-(-q) \Psi^T(q-k) \gamma_0 \Psi(k) \right]. \end{aligned} \quad (29)$$

The counterterm-factors are given by the power series

$$A_\zeta = \sum_{n=1}^{\infty} \frac{Z_\zeta^{(n)}}{\epsilon^n} \text{ with } \zeta \in [1, 6], \quad (30)$$

such that they cancel the divergent $1/\epsilon^n$ contributions from the Feynman diagrams. Due to the $(d - 1)$ -dimensional rotational invariance in the space perpendicular to the Fermi surface, each term in $\mathbf{\Gamma} \cdot \mathbf{K}$ is renormalized in the same way.

Subtracting S_{CT} from the so-called *bare* action S_{bare} , we obtain the renormalized action, which is the *physical* effective action of the theory, re-written in terms of non-divergent quantum parameters. While the bare parameters can be divergent, the physical observables are the renormalized coupling constants, which are determined by the RG equations. The RG flows describe the evolution of the bare couplings as functions of the floating energy scale μe^{-l} (i.e., with respect to an

increasing logarithmic length scale l). To achieve this objective, we first define the bare (or fundamental) action

$$S_{\text{bare}} = \int_{k^B} \bar{\Psi}^B(k^B) i \left[\mathbf{\Gamma} \cdot \mathbf{K}^B + \gamma_{d-1} \left\{ e_k^B + \frac{(k^B)^2}{2} \right\} \right] \Psi^B(k^B) + \int_{k^B} \left[(k_d^B)^2 + \alpha^B e_k^B \right] \phi_+^B(k^B) \phi_-^B(-k^B) - \frac{i e^B}{2} \int_{k^B, q^B} \left[\phi_+^B(q^B) \bar{\Psi}^B(k^B + q^B) \gamma_0 (\bar{\Psi}^B(-k^B))^T + \phi_-^B(-q^B) (\Psi^B(q^B - k^B))^T \gamma_0 \Psi^B(k^B) \right], \quad (31)$$

consisting of the *bare quantities*, where the superscript “ B ” has been used to denote the bare fields, couplings, frequency, and momenta. We now relate the bare quantities to the so-called renormalized quantities (without the superscript “ B ”) via the multiplicative Z_ζ -factors such that

$$S_{\text{bare}} = S + S_{CT}, \quad Z_\zeta = 1 + A_\zeta, \quad (32)$$

$$\mathbf{K}^B = \frac{Z_1}{Z_3} \mathbf{K}, \quad e_k^B = \frac{Z_2}{Z_3} e_k, \quad k_d^B = k_d, \quad \Psi^B(k^B) = Z_\Psi^{1/2} \Psi(k), \quad \phi_\pm^B(k^B) = Z_\phi^{1/2} \phi_\pm, \quad (33)$$

and

$$Z_\Psi = Z_1 \left(\frac{Z_1}{Z_3} \right)^{-d} \left(\frac{Z_2}{Z_3} \right)^{-1}, \quad Z_\phi = Z_4 \left(\frac{Z_1}{Z_3} \right)^{1-d} \left(\frac{Z_2}{Z_3} \right)^{-1}, \quad \tilde{a}^B = Z_5 \left(\frac{Z_1}{Z_3} \right)^{1-d} \left(\frac{Z_2}{Z_3} \right)^{-2}, \\ e^B = Z_e e \mu^{\frac{\epsilon}{2}}, \quad Z_e = \frac{Z_6 \left(\frac{Z_1}{Z_3} \right)^{1-\frac{d}{2}} \left(\frac{Z_2}{Z_3} \right)^{-1/2}}{\sqrt{Z_1} Z_4}. \quad (34)$$

Observing that there exists a freedom to change the renormalization of the fields and the renormalization of momenta without affecting the action, we have exploited it by requiring $k_d^B = k_d$, which is equivalent to measuring the scaling dimensions of all the other quantities relative to the scaling dimension of k_d . S now represents the renormalized action (also known as the Wilsonian effective action) because it consists of the renormalized quantities. Basically, we have written the fundamental action of our theory in two different ways [82], which allows us to subtract off the divergent parts (represented by S_{CT}).

A. RG flow equations from one-loop results

At one-loop order, the divergent contributions are obtained from Eqs.(13) and (19). These lead to

$$Z_1 = 1 - \frac{e^{4/3} \mathcal{U}_1}{(2 - \tilde{a})^{2/3} \epsilon}, \quad Z_2 = 1, \quad Z_3 = 1, \quad Z_4 = 1, \quad Z_5 = 1 - \frac{e^2 \mathcal{U}_2}{\tilde{a} \epsilon}, \quad Z_6 = 1, \\ b = \frac{\pi^{3/4}}{32 \sqrt{2} \Gamma^2(3/4) \Gamma(7/4)}, \quad \mathcal{U}_1 = \frac{\sqrt{2} \Gamma(\frac{5}{4})}{3 \sqrt{3} \pi^{7/4} b^{1/3}}, \quad \mathcal{U}_2 = \frac{1}{32 \pi^{3/4} \Gamma(3/4)}. \quad (35)$$

To this leading order correction, we find that $Z_2 = Z_3$, and they do not get any correction from the loop integrals.

Because $Z_2 = Z_3$, we define a single dynamical critical exponent for the fermions as

$$z = 1 + \frac{\partial \ln \left(\frac{Z_1}{Z_2} \right)}{\partial \ln \mu} = 1 + \frac{\partial \ln \left(\frac{Z_1}{Z_3} \right)}{\partial \ln \mu}. \quad (36)$$

This applies to our one-loop level calculations where the δ_k -part as a whole is not renormalized. Furthermore, the anomalous dimensions for the fermions and the bosons are given by

$$\eta_\psi = \frac{1}{2} \frac{\partial \ln Z_\psi}{\partial \ln \mu} \quad \text{and} \quad \eta_\phi = \frac{1}{2} \frac{\partial \ln Z_\phi}{\partial \ln \mu}, \quad (37)$$

respectively. We also define the beta functions for the two coupling constants as

$$\beta_e = \frac{de}{d \ln \mu} \quad \text{and} \quad \beta_a = \frac{d\tilde{a}}{d \ln \mu}. \quad (38)$$

The sole purpose of the introduction of the *ad hoc* mass scale μ is to regularize the theory, thus eliminating the infinities emerging from the loop integrals of Feynman diagrams. However, since physical quantities must be independent of μ , as

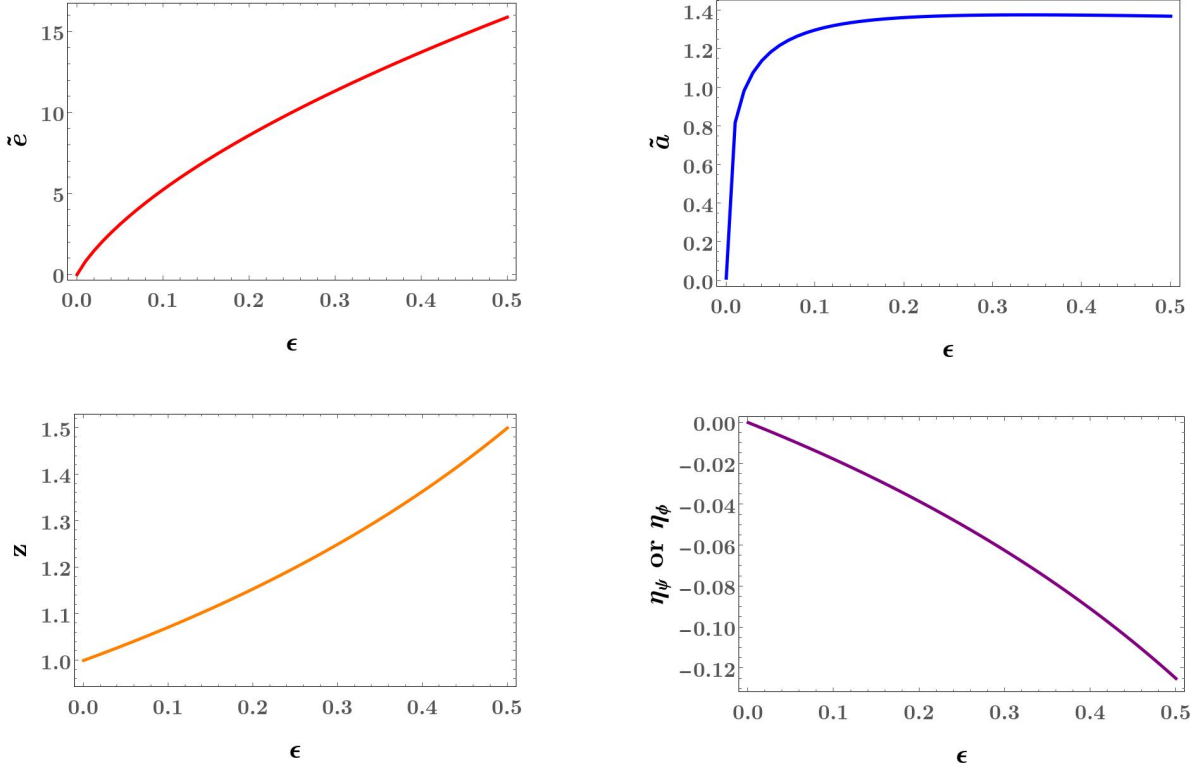


FIG. 3. The fixed-point values of \tilde{z} , \tilde{a} , z , and $\eta_\psi (= \eta_\phi)$, computed numerically from the zeroes of the two beta functions, plotted as functions of $\epsilon \in (0, 1/2]$.

μ is not really a parameter of the fundamental theory, the bare parameters must be independent of it as well. Imposing this condition, as well as the requirement that the regular (i.e., non-singular) parts of the final solutions are of the forms

$$z = z^{(0)}, \quad \eta_\psi = \eta_\psi^{(0)} + \eta_\psi^{(1)} \epsilon, \quad \eta_\phi = \eta_\phi^{(0)} + \eta_\phi^{(1)} \epsilon, \quad \beta_e = \beta_e^{(0)} + \beta_e^{(1)} \epsilon, \quad \beta_a = \beta_a^{(0)} + \beta_a^{(1)} \epsilon, \quad (39)$$

in the limit $\epsilon \rightarrow 0$, we get the following differential equations:

$$\begin{aligned} z &= 1 + \beta_a^{(1)} \frac{\partial Z_1^{(1)}}{\partial \tilde{a}} + \beta_e^{(1)} \frac{\partial Z_1^{(1)}}{\partial e}, \\ \eta_\psi &= \frac{1}{4} \left(5 - 5z + 2 \frac{\partial Z_1^{(1)}}{\partial \tilde{a}} \beta_a^{(1)} + 2 \frac{\partial Z_1^{(1)}}{\partial e} \beta_e^{(1)} \right) + \frac{(z-1)\epsilon}{2}, \quad \eta_\phi = \frac{3-3z}{4} + \frac{(z-1)\epsilon}{2}, \\ \frac{4\beta_e^{(0)}}{e} &= 2 \frac{\partial Z_1^{(1)}}{\partial \tilde{a}} \beta_a^{(1)} - ez \frac{\partial Z_1^{(1)}}{\partial e} + z - 1, \quad \beta_e^{(1)} = -\frac{ez}{2}, \\ \frac{2\beta_a^{(0)}}{\tilde{a}} &= (z-1) \left(3 + 2\tilde{a} \frac{\partial Z_5^{(1)}}{\partial \tilde{a}} \right) - 2 \frac{\partial Z_5^{(1)}}{\partial e} \beta_e^{(1)}, \quad \beta_a^{(1)} = -\tilde{a}(z-1). \end{aligned} \quad (40)$$

The above set of equations have been obtained by (1) demanding that $\frac{d}{d \ln \mu}$ (bare quantity) = 0; (2) plugging in the values from Eqs. (35) and (39); (3) expanding in powers of ϵ ; and (4) matching the coefficients of the regular powers of ϵ in the resulting equations.

Solving the equations, we get

$$\frac{\beta_e^{(0)}}{e} = \frac{3\mathcal{U}_1 \chi \tilde{e}}{2(3\chi^{5/3} - 4\mathcal{U}_1 \tilde{e})}, \quad \beta_e^{(1)} = \frac{2\mathcal{U}_1 \tilde{a} \tilde{e} - 3\chi^{5/3}}{2(3\chi^{5/3} - 4\mathcal{U}_1 \tilde{e})}, \quad (41)$$

$$\frac{\beta_a^{(0)}}{\tilde{e}} = \frac{3\mathcal{U}_1 \chi \tilde{a}}{3\chi^{5/3} - 4\mathcal{U}_1 \tilde{e}} - \mathcal{U}_2 \sqrt{\tilde{e}}, \quad \beta_a^{(1)} = -\frac{2\mathcal{U}_1 \chi \tilde{a}}{3\chi^{5/3} - 4\mathcal{U}_1 \tilde{e}}, \quad (42)$$

$$z = 1 + \frac{2\mathcal{U}_1 \chi \tilde{e}}{3\chi^{5/3} - 4\mathcal{U}_1 \tilde{e}}, \quad \eta_\psi = \eta_\phi = -\frac{\mathcal{U}_1 \chi \tilde{e}}{2(3\chi^{5/3} - 4\mathcal{U}_1 \tilde{e})}, \quad (43)$$

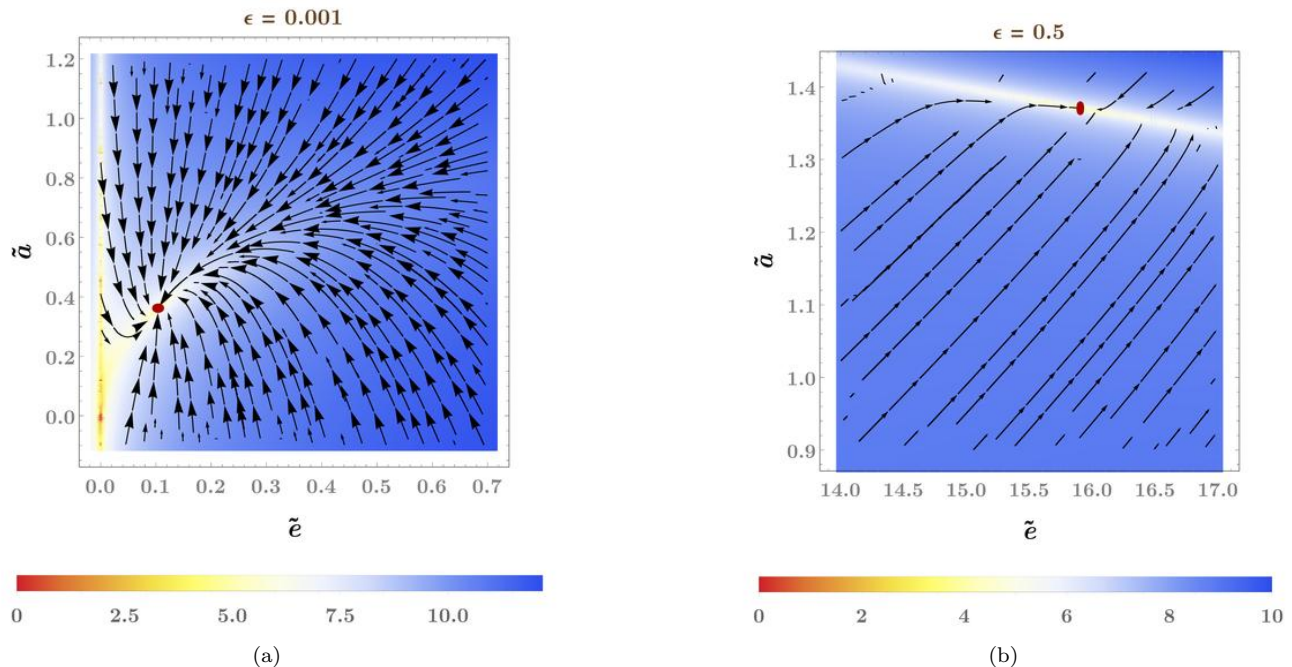


FIG. 4. The RG flows in the \tilde{e} - \tilde{a} plane for two different values of ϵ : (a) $\epsilon = 10^{-3}$ representing the regime around $d = d_c$ and (b) $\epsilon = 1/2$ representing the regime around $d = 2$ (which is the actual/physical dimension of the theory). The red disc represents the IR-stable fixed point in each case. The contour-shading (with the values shown in the plot-legends) corresponds to the natural logarithm of the norm of the flow vector field $\{-\beta_e, -\beta_a\}$ plus (a) 17 and (b) 8, respectively.

where

$$\tilde{e} = e^{4/3} \text{ and } \chi = 2 - \tilde{a}. \quad (44)$$

Since we are interested in the behaviour at the IR energy scales, we determine the RG flows with respect to the logarithmic length scale l , which are given by the derivatives

$$\frac{de}{dl} \equiv -\beta_e \text{ and } \frac{d\tilde{a}}{dl} \equiv -\beta_a, \quad (45)$$

for the two coupling constants e and \tilde{a} , respectively.

B. Stable fixed points

The fixed points of the theory are obtained as the points where the two beta functions, viz. β_e and β_a , go to zero simultaneously. The nomenclature originates from the fact that these are the *equilibrium points* of the differential equations describing the RG flows in the space of the two coupling constants, e and \tilde{a} . Due to the complicated form of the beta functions, it is not feasible to obtain closed-form expressions for these fixed points. Hence, we find their values numerically for a given value of ϵ . In order to determine the stability of a fixed point, one needs to figure out whether the flow lines (in the IR), given by the vector field with the components $\{-\beta_e, -\beta_a\}$ in the \tilde{e} - \tilde{a} plane, are towards or away from it. Accordingly, they are classified as stable or unstable. The values of z , η_ψ , and η_ϕ at the stable fixed points, as functions of ϵ , are shown in Fig. 3. In the range $\epsilon \in (0, 1/2]$, we find precisely one stable fixed point for each value of ϵ . The stable nature of these fixed points has been illustrated by the RG flows for $\epsilon = 10^{-3}$ and $\epsilon = 1/2$ in Fig. 4, which is obvious from the fact that the RG flow trajectories in each subfigure converge towards the fixed point while flowing from a high value of the floating mass scale to lower and lower values.

Since $Z_2 = Z_3 = 1$ at the one-loop order, we do not find any flattening of the Fermi surface at the hot-spots, unlike the interpretation of Ref. [77], where the authors performed the RG using the pole of Σ_2 at $d = 3/2$. Furthermore, we would like to point out that both the fermionic and the bosonic anomalous dimensions remain equal, each taking a negative value (see the last panel of Fig. 3) in the range $\epsilon \in (0, 1/2]$, unlike the results found in Ref. [77].

V. Discussions and outlook

In this paper, we have revisited the QFT of the quantum critical point emerging at the continuous phase transition from a normal metal phase to an ordered phase involving an incommensurate CDW modulation. In our one-loop computations, we have used a dressed boson propagator by including the Landau-damping correction Π_{LD} , which is instrumental in inducing the non-Fermi liquid behaviour with a characteristic scaling of $\text{sgn}(k_0)|k_0|^{2/3}$ for the fermion self-energy [19–21, 52–54, 83]. In Ref. [77], the authors computed the fermion self-energy $\Sigma(k)$ by assuming the *ad hoc* form of the boson-self energy $\tilde{\Pi}(q)$ to be $\propto -q_{d-1}$, which they argued is generated in RG due to symmetry arguments. However, a careful analysis shows that the RG procedure generates a term proportional to e_k and, additionally, terms with Landau damping [cf. Eq. (13)]. As a consequence of not including the all-important Landau-damped term in the dressed bosonic propagator, they did not obtain any contribution in $\Sigma(k)$ proportional to $\Gamma \cdot \mathbf{K}$ and, hence, missed the crucial $\text{sgn}(k_0)|k_0|^{2/3}$ -dependence at $d = 2$. They concluded that the correct frequency-dependence would show up at two-loop order. Furthermore, Halbinger *et al.* included the part proportional to γ_{d-1} in the one-loop fermion self-energy in the counterterms, which leads to their conclusion of the flattening of the Fermi surface at the hot-spots (as found in the RPA calculations of Ref. [76]). However, that term has a factor of $\Gamma(3/2 - d)$, which first blows up at $d = 3/2$ — hence, it should not contribute to the beta-functions for the flows towards IR, when d_c is equal to $5/2$. Their integrals are actually somewhat similar to the scenario for our I_3 calculation, and we have argued in detail why that term should not be included while computing the RG flows.

While we have addressed here the behaviour of a system with two hot-spots in the incommensurate CDW setting in two spatial dimensions, it will be worthwhile to extend it to the case of three dimensions [84], where we expect a marginal Fermi liquid behaviour, analogous to the results found in Refs. [20, 21, 53]. Another interesting direction to investigate is the scenario when the Fermi surface harbours two pairs of hot-spots [85]. Last, but not the least, we would like to compute the nature of superconducting instabilities in the presence of these critical CDW bosons, utilizing the RG set-ups constructed in Refs. [23, 59].

Acknowledgments

We are grateful for useful discussions with Sung-Sik Lee, Ashoke Sen, and Dimitri Pimenov. We thank Peng Rao for participating in the initial stages of the calculations. This research, leading to the results reported, has received funding from the European Union’s Horizon 2020 research and innovation programme under the Marie Skłodowska-Curie grant agreement number 754340.

Appendix: Details of calculating the b -dependent part of Σ_2

In this appendix, we compute the b -dependent part of the fermion self-energy contribution from Σ_2 [cf. Eqs. (16) and (18)]. Starting with Eq. (24), we define

$$\Sigma_2(\mathbf{0}, k_d, k_{d-1}) = e^2 \mu^{x_e} (I_4 + I_5), \quad (46)$$

where

$$I_4 = \int_{q, e_q < 0} \frac{\delta_{q-k}}{\mathbf{Q}^2 + \delta_{q-k}^2} \times \frac{1}{q_d^2 + \tilde{a} e_q + e^2 \mu^{x_e} b |\mathbf{Q}|^{d-1} / \sqrt{|e_q|}}, \quad (47)$$

and

$$I_5 = \int_{q, e_q > 0} \frac{\delta_{q-k}}{\mathbf{Q}^2 + \delta_{q-k}^2} \times \frac{1}{q_d^2 + \tilde{a} e_q}. \quad (48)$$

We note that $\delta_{q-k} = e_q + e_{-k} + k_d^2/2 + q_d^2/2 - 2k_q q_d$. Since the part I_5 is included in I_3 , whose computation has been detailed in the main text itself, we focus only on I_4 here.

To simplify the calculations a bit, we set k_d to zero to obtain

$$\begin{aligned} I_4 &= \int_{q, e_q > 0} \frac{q_d^2/2 - e_q - k_{d-1}}{\mathbf{Q}^2 + (q_d^2/2 - e_q - k_{d-1})^2} \times \frac{1}{q_d^2 - \tilde{a} e_q + e^2 \mu^{x_e} b |\mathbf{Q}|^{d-1} / \sqrt{e_q}} \\ &= \int_0^\infty \frac{du}{\sqrt{u/2}} \int_0^\infty de_q \int_{-\infty}^\infty \frac{d^{d-1} \mathbf{Q}}{(2\pi)^{d+1}} \frac{u - e_q - k_{d-1}}{|\mathbf{Q}|^2 + (u - e_q - k_{d-1})^2} \frac{1}{2u - \tilde{a} e_q + e^2 \mu^{x_e} b |\mathbf{Q}|^{d-1} / \sqrt{e_q}} \quad [\text{where } 2u = q_d^2]. \end{aligned} \quad (49)$$

We observe that the first factor of the integrand forces the dominant contribution to be concentrated around the region $|\mathbf{Q}| \sim 0$ and $u \sim e_q + k_{d-1}$. As for the second factor, the dominant contribution comes from $e_q \sim |\mathbf{Q}|^{2(d-1)/3}$. Hence, we

can substitute $u \sim e_q + k_{d-1}$ in the \sqrt{u} factor (in the overall denominator) and the $2u$ term (in the denominator of the second factor), and extend the lower limit of the integral over u to $-\infty$. This leads to

$$I_4 \simeq \int_0^\infty \frac{du}{\sqrt{e_q + k_{d-1}}} \int_0^\infty de_q \int_{-\infty}^\infty \frac{d^{d-1}\mathbf{Q}}{(2\pi)^{d+1}} \frac{u - e_q - k_{d-1}}{|\mathbf{Q}|^2 + (u - e_q - k_{d-1})^2} \frac{\sqrt{2}}{(2 - \tilde{a})e_q + 2k_{d-1} + e^2 \mu^{x_e} b |\mathbf{Q}|^{d-1} / \sqrt{e_q}} = 0. \quad (50)$$

Hence, to leading order, the I_4 integral vanishes, and there remains no b -dependent term.

-
- [1] T. Holstein, R. E. Norton, and P. Pincus, de Haas-van Alphen effect and the specific heat of an electron gas, *Phys. Rev. B* **8**, 2649 (1973).
- [2] M. A. Metlitski and S. Sachdev, Quantum phase transitions of metals in two spatial dimensions. I. Ising-nematic order, *Phys. Rev. B* **82**, 075127 (2010).
- [3] V. Oganesyan, S. A. Kivelson, and E. Fradkin, Quantum theory of a nematic Fermi fluid, *Phys. Rev. B* **64**, 195109 (2001).
- [4] W. Metzner, D. Rohe, and S. Andergassen, Soft Fermi surfaces and breakdown of Fermi-liquid behavior, *Phys. Rev. Lett.* **91**, 066402 (2003).
- [5] L. Dell'Anna and W. Metzner, Fermi surface fluctuations and single electron excitations near Pomeranchuk instability in two dimensions, *Phys. Rev. B* **73**, 045127 (2006).
- [6] H.-Y. Kee, E. H. Kim, and C.-H. Chung, Signatures of an electronic nematic phase at the isotropic-nematic phase transition, *Phys. Rev. B* **68**, 245109 (2003).
- [7] M. J. Lawler, D. G. Barci, V. Fernández, E. Fradkin, and L. Oxman, Nonperturbative behavior of the quantum phase transition to a nematic Fermi fluid, *Phys. Rev. B* **73**, 085101 (2006).
- [8] J. Rech, C. Pépin, and A. V. Chubukov, Quantum critical behavior in itinerant electron systems: Eliashberg theory and instability of a ferromagnetic quantum critical point, *Phys. Rev. B* **74**, 195126 (2006).
- [9] P. Wölfle and A. Rosch, Fermi liquid near a quantum critical point, *Journal of Low Temperature Physics* **147**, 165 (2007).
- [10] D. L. Maslov and A. V. Chubukov, Fermi liquid near Pomeranchuk quantum criticality, *Phys. Rev. B* **81**, 045110 (2010).
- [11] J. Quintanilla and A. J. Schofield, Pomeranchuk and topological Fermi surface instabilities from central interactions, *Phys. Rev. B* **74**, 115126 (2006).
- [12] H. Yamase and H. Kohno, Instability toward formation of quasi-one-dimensional Fermi surface in two-dimensional t-J model, *Journal of the Physical Society of Japan* **69**, 2151 (2000).
- [13] H. Yamase, V. Oganesyan, and W. Metzner, Mean-field theory for symmetry-breaking Fermi surface deformations on a square lattice, *Phys. Rev. B* **72**, 035114 (2005).
- [14] C. J. Halboth and W. Metzner, d-wave superconductivity and Pomeranchuk instability in the two-dimensional Hubbard model, *Phys. Rev. Lett.* **85**, 5162 (2000).
- [15] P. Jakubczyk, P. Strack, A. A. Katanin, and W. Metzner, Renormalization group for phases with broken discrete symmetry near quantum critical points, *Phys. Rev. B* **77**, 195120 (2008).
- [16] M. Zacharias, P. Wölfle, and M. Garst, Multiscale quantum criticality: Pomeranchuk instability in isotropic metals, *Phys. Rev. B* **80**, 165116 (2009).
- [17] E.-A. Kim, M. J. Lawler, P. Oreto, S. Sachdev, E. Fradkin, and S. A. Kivelson, Theory of the nodal nematic quantum phase transition in superconductors, *Phys. Rev. B* **77**, 184514 (2008).
- [18] Y. Huh and S. Sachdev, Renormalization group theory of nematic ordering in d-wave superconductors, *Phys. Rev. B* **78**, 064512 (2008).
- [19] D. Dalidovich and S.-S. Lee, Perturbative non-Fermi liquids from dimensional regularization, *Phys. Rev. B* **88**, 245106 (2013).
- [20] I. Mandal and S.-S. Lee, Ultraviolet/infrared mixing in non-Fermi liquids, *Phys. Rev. B* **92**, 035141 (2015).
- [21] I. Mandal, UV/IR mixing in non-Fermi liquids: higher-loop corrections in different energy ranges, *The European Physical Journal B* **89**, 278 (2016).
- [22] A. Eberlein, I. Mandal, and S. Sachdev, Hyperscaling violation at the Ising-nematic quantum critical point in two-dimensional metals, *Phys. Rev. B* **94**, 045133 (2016).
- [23] I. Mandal, Superconducting instability in non-Fermi liquids, *Phys. Rev. B* **94**, 115138 (2016).
- [24] I. Mandal, Erratum: Superconducting instability in non-Fermi liquids [Phys. Rev. B 94, 115138 (2016)], *Phys. Rev. B* **109**, 079902 (2024).
- [25] M. A. Metlitski and S. Sachdev, Quantum phase transitions of metals in two spatial dimensions. II. Spin density wave order, *Phys. Rev. B* **82**, 075128 (2010).
- [26] A. Abanov and A. Chubukov, Anomalous scaling at the quantum critical point in itinerant antiferromagnets, *Physical Review Letters* **93**, 255702 (2004).
- [27] A. Abanov and A. V. Chubukov, Spin-Fermion model near the quantum critical point: One-loop renormalization group results, *Physical Review Letters* **84**, 5608 (2000).
- [28] S. Sur and S.-S. Lee, Quasilocal strange metal, *Phys. Rev. B* **91**, 125136 (2015).
- [29] I. Mandal, Scaling behaviour and superconducting instability in anisotropic non-Fermi liquids, *Annals of Physics* **376**, 89 (2017).
- [30] A. Schliefl, P. Lunts, and S.-S. Lee, Exact critical exponents for the antiferromagnetic quantum critical metal in two dimensions, *Phys. Rev. X* **7**, 021010 (2017).
- [31] P. Lunts, A. Schliefl, and S.-S. Lee, Emergence of a control parameter for the antiferromagnetic quantum critical metal, *Phys. Rev. B* **95**, 245109 (2017).

- [32] G. Baskaran and P. W. Anderson, Gauge theory of high-temperature superconductors and strongly correlated Fermi systems, *Phys. Rev. B* **37**, 580 (1988).
- [33] L. B. Ioffe and A. I. Larkin, Gapless fermions and gauge fields in dielectrics, *Phys. Rev. B* **39**, 8988 (1989).
- [34] P. A. Lee, Gauge field, Aharonov-Bohm flux, and high- T_c superconductivity, *Phys. Rev. Lett.* **63**, 680 (1989).
- [35] P. A. Lee and N. Nagaosa, Gauge theory of the normal state of high- T_c superconductors, *Phys. Rev. B* **46**, 5621 (1992).
- [36] B. Blok and H. Monien, Gauge theories of high- T_c superconductors, *Phys. Rev. B* **47**, 3454 (1993).
- [37] M. U. Ubbens and P. A. Lee, Superconductivity phase diagram in the gauge-field description of the t-J model, *Phys. Rev. B* **49**, 6853 (1994).
- [38] C. Nayak and F. Wilczek, Non-Fermi liquid fixed point in $2 + 1$ dimensions, *Nuclear Physics B* **417**, 359 (1994).
- [39] S. Chakravarty, R. E. Norton, and O. F. Syljuåsen, Transverse gauge interactions and the vanquished Fermi liquid, *Physical Review Letters* **74**, 1423 (1995).
- [40] M. Y. Reizer, Relativistic effects in the electron density of states, specific heat, and the electron spectrum of normal metals, *Phys. Rev. B* **40**, 11571 (1989).
- [41] B. I. Halperin, P. A. Lee, and N. Read, Theory of the half-filled Landau level, *Phys. Rev. B* **47**, 7312 (1993).
- [42] J. Polchinski, Low-energy dynamics of the spin-gauge system, *Nuclear Physics B* **422**, 617 (1994).
- [43] B. L. Altshuler, L. B. Ioffe, and A. J. Millis, Low-energy properties of fermions with singular interactions, *Phys. Rev. B* **50**, 14048 (1994).
- [44] C. Nayak and F. Wilczek, Renormalization group approach to low temperature properties of a non-Fermi liquid metal, *Nuclear Physics B* **430**, 534 (1994).
- [45] S.-S. Lee, Low-energy effective theory of Fermi surface coupled with U(1) gauge field in $2 + 1$ dimensions, *Phys. Rev. B* **80**, 165102 (2009).
- [46] D. F. Mross, J. McGreevy, H. Liu, and T. Senthil, Controlled expansion for certain non-Fermi-liquid metals, *Phys. Rev. B* **82**, 045121 (2010).
- [47] H.-C. Jiang, M. S. Block, R. V. Mishmash, J. R. Garrison, D. N. Sheng, O. I. Motrunich, and M. P. A. Fisher, Non-Fermi-liquid d-wave metal phase of strongly interacting electrons, *Nature (London)* **493**, 39 (2013).
- [48] S. B. Chung, I. Mandal, S. Raghu, and S. Chakravarty, Higher angular momentum pairing from transverse gauge interactions, *Phys. Rev. B* **88**, 045127 (2013).
- [49] Z. Wang, I. Mandal, S. B. Chung, and S. Chakravarty, Pairing in half-filled Landau level, *Annals of Physics* **351**, 727 (2014).
- [50] S. Sur and S.-S. Lee, Chiral non-Fermi liquids, *Phys. Rev. B* **90**, 045121 (2014).
- [51] S.-S. Lee, Recent developments in non-Fermi liquid theory, *Annual Review of Condensed Matter Physics* **9**, 227–244 (2018).
- [52] D. Pimenov, I. Mandal, F. Piazza, and M. Punk, Non-Fermi liquid at the FFLO quantum critical point, *Phys. Rev. B* **98**, 024510 (2018).
- [53] I. Mandal, Critical Fermi surfaces in generic dimensions arising from transverse gauge field interactions, *Phys. Rev. Research* **2**, 043277 (2020).
- [54] I. Mandal and R. M. Fernandes, Valley-polarized nematic order in twisted moiré systems: In-plane orbital magnetism and crossover from non-Fermi liquid to Fermi liquid, *Phys. Rev. B* **107**, 125142 (2023).
- [55] A. A. Abrikosov, Calculation of critical indices for zero-gap semiconductors, *Journal of Experimental and Theoretical Physics* **39**, 709 (1974).
- [56] E.-G. Moon, C. Xu, Y. B. Kim, and L. Balents, Non-Fermi-liquid and topological states with strong spin-orbit coupling, *Phys. Rev. Lett.* **111**, 206401 (2013).
- [57] R. M. Nandkishore and S. A. Parameswaran, Disorder-driven destruction of a non-Fermi liquid semimetal studied by renormalization group analysis, *Phys. Rev. B* **95**, 205106 (2017).
- [58] I. Mandal and R. M. Nandkishore, Interplay of Coulomb interactions and disorder in three-dimensional quadratic band crossings without time-reversal symmetry and with unequal masses for conduction and valence bands, *Phys. Rev. B* **97**, 125121 (2018).
- [59] I. Mandal, Fate of superconductivity in three-dimensional disordered Luttinger semimetals, *Annals of Physics* **392**, 179 (2018).
- [60] I. Mandal and H. Freire, Transport in the non-Fermi liquid phase of isotropic Luttinger semimetals, *Phys. Rev. B* **103**, 195116 (2021).
- [61] H. Freire and I. Mandal, Thermoelectric and thermal properties of the weakly disordered non-Fermi liquid phase of Luttinger semimetals, *Physics Letters A* **407**, 127470 (2021).
- [62] I. Mandal and H. Freire, Raman response and shear viscosity in the non-Fermi liquid phase of Luttinger semimetals, *Journal of Physics: Condensed Matter* **34**, 275604 (2022).
- [63] B. Roy, M. P. Kennett, K. Yang, and V. Juričić, From birefringent electrons to a marginal or non-Fermi liquid of relativistic spin-1/2 fermions: An emergent superuniversality, *Phys. Rev. Lett.* **121**, 157602 (2018).
- [64] I. Mandal, Robust marginal Fermi liquid in birefringent semimetals, *Physics Letters A* **418**, 127707 (2021).
- [65] I. Mandal and H. Freire, Transport properties in non-Fermi liquid phases of nodal-point semimetals, arXiv e-prints (2024), [arXiv:2404.08635 \[cond-mat.str-el\]](https://arxiv.org/abs/2404.08635).
- [66] H. J. Schulz, Incommensurate antiferromagnetism in the two-dimensional Hubbard model, *Phys. Rev. Lett.* **64**, 1445 (1990).
- [67] P. A. Igoshev, M. A. Timirgazin, A. A. Katanin, A. K. Arzhnikov, and V. Y. Irkhin, Incommensurate magnetic order and phase separation in the two-dimensional Hubbard model with nearest- and next-nearest-neighbor hopping, *Phys. Rev. B* **81**, 094407 (2010).
- [68] S. Sachdev and R. La Placa, Bond order in two-dimensional metals with antiferromagnetic exchange interactions, *Phys. Rev. Lett.* **111**, 027202 (2013).
- [69] F. D. S. J.A. Wilson and S. Mahajan, Charge-density waves and superlattices in the metallic layered transition metal dichalcogenides, *Advances in Physics* **24**, 117 (1975).
- [70] G. Scholz, O. Singh, R. Frindt, and A. Curzon, Charge density wave commensurability in 2H-TaS_2 and Ag_xTaS_2 , *Solid State Communications* **44**, 1455 (1982).
- [71] P. Chen, W. W. Pai, Y.-H. Chan, V. Madhavan, M. Y. Chou, S.-K. Mo, A.-V. Fedorov, and T.-C. Chiang, Unique gap structure

- and symmetry of the charge density wave in single-layer VSe₂, *Phys. Rev. Lett.* **121**, 196402 (2018).
- [72] G.-H. Gweon, J. D. Denlinger, J. A. Clack, J. W. Allen, C. G. Olson, E. DiMasi, M. C. Aronson, B. Foran, and S. Lee, Direct observation of complete Fermi surface, imperfect nesting, and gap anisotropy in the high-temperature incommensurate charge-density-wave compound SmTe₃, *Phys. Rev. Lett.* **81**, 886 (1998).
- [73] A. Fang, N. Ru, I. R. Fisher, and A. Kapitulnik, STM studies of TbTe₃: Evidence for a fully incommensurate charge density wave, *Phys. Rev. Lett.* **99**, 046401 (2007).
- [74] Y. Feng, J. van Wezel, J. Wang, F. Flicker, D. M. Silevitch, P. B. Littlewood, and T. F. Rosenbaum, Itinerant density wave instabilities at classical and quantum critical points, *Nature Physics* **11**, 865 (2015).
- [75] T. Holder and W. Metzner, Non-Fermi-liquid behavior at the onset of incommensurate $2k_F$ charge- or spin-density wave order in two dimensions, *Phys. Rev. B* **90**, 161106 (2014).
- [76] J. Sýkora, T. Holder, and W. Metzner, Fluctuation effects at the onset of the $2k_F$ density wave order with one pair of hot spots in two-dimensional metals, *Phys. Rev. B* **97**, 155159 (2018).
- [77] J. Halbinger, D. Pimenov, and M. Punk, Incommensurate $2k_F$ density wave quantum criticality in two-dimensional metals, *Phys. Rev. B* **99**, 195102 (2019).
- [78] T. Senthil and R. Shankar, Fermi surfaces in general codimension and a new controlled nontrivial fixed point, *Phys. Rev. Lett.* **102**, 046406 (2009).
- [79] M. A. Metlitski, D. F. Mross, S. Sachdev, and T. Senthil, Cooper pairing in non-Fermi liquids, *Phys. Rev. B* **91**, 115111 (2015).
- [80] G. 't Hooft, Dimensional regularization and the renormalization group, *Nuclear Physics B* **61**, 455 (1973).
- [81] S. Weinberg, New approach to the renormalization group, *Phys. Rev. D* **8**, 3497 (1973).
- [82] M. Srednicki, *Quantum field theory* (Cambridge University Press, 2007).
- [83] P. Rao and F. Piazza, Non-Fermi-liquid behavior from cavity electromagnetic vacuum fluctuations at the superradiant transition, *Phys. Rev. Lett.* **130**, 083603 (2023).
- [84] T. Schäfer, A. A. Katanin, K. Held, and A. Toschi, Interplay of correlations and kohn anomalies in three dimensions: Quantum criticality with a twist, *Phys. Rev. Lett.* **119**, 046402 (2017).
- [85] J. Sýkora and W. Metzner, Fluctuation effects at the onset of $2k_F$ density wave order with two pairs of hot spots in two-dimensional metals, *Phys. Rev. B* **104**, 125123 (2021).